Journal of Mechanical Engineering and Sciences
ISSN (Print): 2289-4659; e-ISSN: 2231-8380
Volume 12, Issue 2, pp. 3724-3737, June 2018

DOI:https://doi.org/10.15282/jmes.12.2.2018.17.0329

The effect of 10μm microchannel on thermo-hydraulic performance for single-phase flow in semi-circular cross-section serpentine

S.M. Chan[1], K.H. Chong[1*] and Basil T. Wong[1]

[1]Department of Mechanical Engineering, Faculty of Engineering, Computer and Science, Swinburne University of Technology Sarawak Campus, Jalan Simpang Tiga, 93300 Kuching, Sarawak, Malaysia
Phone:+6082260623; Fax:+6082260813
[*]Email: kchong@swinburne.edu.my

ABSTRACT

A microchannel heat exchanger, which offers various engineering applications, such as heating, ventilation and air-conditioning, is increasingly important due to its advantages in cost reduction for material, fabrication, and physical size. The current nanotechnology impedes the fabrication of microchannel hydraulic diameter at 10 μm and below; however, with rigorous research on nanotechnology, a smaller hydraulic diameter relative to the current microchannel is anticipated. This study simulated the effect of 10 μm transitional microchannel on thermo-hydraulic performance for single-phase flow in semi-circular cross-section serpentine, in which the boundary condition for wall temperature is constant—350 K. Its results show that the Dean vortices increase with Reynolds number, leading to a heat transfer enhancement in the region of the serpentine bend. For Reynolds number of 175, the achieved heat transfer coefficient is 768673.71 kJ/m^{2}K, which is superior to what has been reported in other literature; therefore, the study suggests that a hydraulic diameter channel of 10 μm could greatly improve the heat transfer performance. In addition, it infers the suitability of hydraulic diameter channel of 10 μm for single-phase flow in semi-circular cross-section serpentine transitional microchannel.

Keywords: Thermo-hydraulic; Single-phase flow; Semi-circular; Serpentine; Microchannel.

INTRODUCTION

Microchannel offers a variety of engineering, biomedical application in industries, and one of the critical factors to enhance thermo-hydraulic performance in microchannel is its hydraulic diameter. There have been many studies on various microchannel geometry with water as working fluid where hydraulic diameter is above 10 μm, for example [1-25]. Given that the microchannel for 1-phase flow in semi-circular cross-section transitional serpentine, with hydraulic diameter below 10 μm, is limited, due to current fabrication techniques, it is, however, a challenge that can be overcome in the future, as a result of rigorous research and development in microfluidic area. The development of microfluids appeared in 1980s with Tuckerman and Pease [7]. Defined as a channel's dimension in the range of greater or equal to 200 μm and less than 10 μm, where transitional microchannel is greater or equal to 10 μm [26], a microchannel has direct impact on micro-electro mechanical systems, microelectronic cooling and

biomedical devices. Human blood vessels with a diameter range between 10 and 15 µm mainly involves heat and mass transfer [27].

Microchannel could have 1-phase flow and 2-phase flow, where 1-phase flow consists only of single fluid flow; 2-phase flow consists of two-phase fluid (e.g. gas and liquid). According to Kandlikar and Grande, for 1-phase (incompressible) channel, a diameter up to 200 µm will be subjected to the same physical change as that of conventional channel (hydraulic diameter more than 3 µm) [26]. The study on 1-phase flow is a commonly encountered phenomenon in many applications. Most of the experimental research work on a hydraulic diameter above 10 µm, due to the limited technology to manufacture microchannel below 10 µm, which leads to limited simulation work on microchannel with hydraulic diameter of 10 µm or below. Therefore, this study sets to explore the thermo-hydraulic performance for 1-phase flow in semi-circular cross-section serpentine transitional microchannel with hydraulic diameter of 10 µm.

Serpentine microchannel provides bend that promotes greater heat transfer enhancement (HTE) as a result of intensified mixing at the bend region. Some researchers studied the impact of microchannel bend on HTE with various radii of curvature [28-29]. Besides the radius of curvature, Reynolds number has a significant impact on HTE also. An increase in Reynolds number would increase the Dean vortices at serpentine bends. Figure 1 outlines the semi-circular cross section of transitional serpentine in this work; it is a repetitive module representing the whole compact microchannel heat exchanger. This module is represented by 2L, radius of curvature (R_c) and channel diameter (d). In this research, the effect of Reynolds number on HTE and pressure drop are confined to fully developed flow and constant wall (T_w). The aforementioned conditions replicate the typical operating condition in microchannel heat exchanger. Other variables such as (L) and radius of curvature remain constant throughout the study.

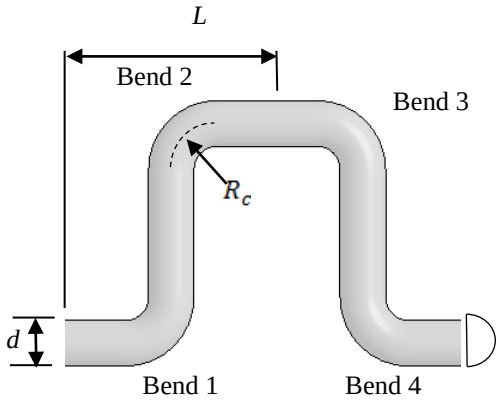

Figure 1. Semi-circular cross section of transitional serpentine.

The following section reviews the important factors on thermo-hydraulic performance in microchannel heat exchanger.

Straight Channel Nusselt Number

Ratio of convective to conductive heat transfer across a boundary is the definition of Nusselt number (Nu). It is characterised as the following,

$$Nu = hD_h / k_f \quad (1)$$

where h, D_h and k_f are convective heat transfer, hydraulic diameter and fluid thermal conductivity, respectively. For semi-circular cross-section, D_h is defined by Eq. (2)

$$D_h = (d/1) + (2/\pi) \quad (2)$$

Nusselt number of a semi-circular straight channel in the latest finding is displayed in Table 1. $H2$ and T_w are constant wall heat flux and constant wall temperature, respectively.

Table 1. Latest findings of Nusselt numbers

Nusselt number (Nu)		Reference
$H2$	T_w	
-	3.221	[30]
-	3.285	[28]
2.921	3.323	[28]
2.923	3.323	[31]
2.925	3.326	[32]

Heat Transfer Enhancement and Pressure Drop

To investigate the enhancement of different path layout compared to straight channel, Venter proposed the Nusselt number of a serpentine channel compared to a straight channel [30]. The enhancement factor (e_{Nu}) is defined as the following.

$$e_{Nu} = Nu_{path\ shape} / Nu_{straight} \quad (3)$$

The same approach is used to measure the pressure drop penalty (e_f) of different path layouts. The pressure drop penalty (e_f) of the serpentine channel relative to a straight channel is given below.

$$e_f = f_{serpentine} / f_{straight} \quad (4)$$

Flow Behaviour of Serpentine Channel

The rate of convection heat transfer within the serpentine channel is dependent on the characteristics of fluid flow. Channel bend could enhance the rate of convection heat transfer. Moreover, in this study, there are four bends for a serpentine path layout with each having different HTE. At bends 1 and 4, the fluid rotates in an anti-clockwise direction, whereas, at bends 2 and 3, it rotates in a clockwise direction (Figure 1). The rotational direction alternates after every second bend, causing the bends to have different performance of heat transfer. After the fluid flow through bend 1, the vortices rotate in a reversed direction in the vicinity of bend 2, causing it to be weak in heat transfer. Similarly, the reversal of direction in bend 4 after bend 3 causes a reduction in

heat transfer. As bends 2 and 3 have the same rotation direction, the strength of the vortices is enhanced within the passage, which causes bend 3 to have good heat transfer performance. Likewise, the rotational direction of bends 4 and 1 is in the same sense, which causes HTE to be better in bend 1. Therefore, bends 1 and 3 are known as curvature reinforcing bends and bends 2 and 4 are known as cancelling bends.

The rotation flow of fluid is called Dean Vortices. The characterisation of Dean vortices (D_n) is expressed as follows:

$$D_n = R_e\left(d/R_c\right)^{1/2} \tag{5}$$

The above equation is used to indicate the importance of inertial and centrifugal forces relative to viscous forces. At low Dean Number or Reynolds number, the flow tends towards the straight channel solution, where there will be no secondary flow because the viscous forces of fluid are larger than the inertial forces. Therefore, the viscous force suppresses the formation of secondary flow, which is consistent with low heat transfer enhancement and pressure drop at low Reynolds number. However, when the Reynolds number increases, the inertial forces become larger than the viscous forces, and a single vortex is developed. The flow complexity, as well as the number and strength of vortices, increase with the Reynolds number.

Effect of Geometrical Parameters

Rosaguti et al. verified the parameters that affect heat transfer enhancement and pressure drop penalty along the serpentine path layout: L/d and R_c/d [28]. To determine the effect, one of the parameters will be fixed when increasing another parameter.

By increasing the value of L/d at fixed R_c/d, both the heat transfer enhancement and pressure drop penalty decrease; the straight passage of the channel becomes longer when L/d is increased, which stabilises the flow and, subsequently, reduces the mixing of fluids. Rosaguti et al. stated that the flow development occurs in this longer section, causing the relaxation of HTE towards unity, in other words, towards the value for the straight channel flow [28]. Therefore, as the straight section between bends increases, the value of HTE decreases and the differences of enhancement factor between reinforcing bends and cancelling bends are reduced also by increasing L/d .

Moreover, the radius of curvature has significant effects on the enhancement factor and pressure drop penalty. A decrease in the radius of curvature (R_c/d) leads to greater heat transfer enhancement and pressure drop penalty; at lower values of radius of curvature, the bends are sharper, which promotes the formation of Dean vortices and flow separation in the bends' vicinity. The formation of flow separation and Dean vortices can cause the pressure drop to increase around the bends. The Equation (5) can be employed to determine the strength of vortices by substituting the value of R_c/d into the equation. Furthermore, based on the path layout of the channel, the effect of radius of curvature on heat transfer enhancement can be explained. When the value of R_c/d decreases, the bends become sharper and the vortices become more complex, which, in turn, promotes fluid mixing and increases HTE at miter bends. However, when the

value of R_c/d increases, the bends become rounded and fewer vortexes emerge in the bends' vicinity, which contributes to a lower enhancement factor.

Effect of Reynolds Number

The effects of Reynolds number on heat transfer enhancement and relative pressure drop penalty have been proven by various studies. Rosaguti et al. reported that heat transfer and pressure drop increase with the value of Reynolds number [28], whose consequence is attributed to the velocity of fluid flow being increased when the Reynolds number is increased. The effect of Reynolds number (R_e) on fluid flow velocity can be determined with Equation (6):

$$R_e = \rho V D_h / \mu \tag{6}$$

On one hand, at low Reynolds numbers, the thermal-hydraulic performance of the serpentine channel is low and the viscous forces suppress the secondary flow; on the other hand, at high Reynolds numbers, it causes the strength of Dean vortices to increase, which is consistent with the increase of heat transfer enhancement and pressure drop penalty. At low Reynolds numbers, the vortex is weak, due to flow development occurring within the straight section of the serpentine channel. As the Reynolds number increases, the strength of the vortex increases also, thus, allowing it to survive into the straight section. The strength of the vortex, being dependent on the location of the bends, is the highest at bends 2 and 4, the cancelling bends. Therefore, at high Reynolds number, the vortex strength is high, which in turn increases the distance it can progress into the straight section.

METHODOLOGY

In this study, the numerical analysis was accomplished with ANSYS FLUENT 16.1 [33]. All the calculations are solved using the second-order bounded differencing scheme for the convective terms.

The simulation was accomplished by setting the entrance channel as velocity inlet, and the exit channel as atmospheric pressure outlet, which was applied on both straight and serpentine path layouts. A rotational periodic type boundary condition was applied for the serpentine layout. The wall temperature was set constant at 350 K, and the fluid inlet channel temperature was set at 300 K. There were three units of serpentine path layout, of which the central unit is where fully developed flow occurs. Twenty planes were created within the central unit to determine the Nusselt number of straight and serpentine microchannels (Figure 6). The average bulk fluid temperature and the local wall heat flux were determined from the created planes. The average bulk fluid temperature (T_b) is defined as follows:

$$T_b = \left(T_{\max} + T_{\min}\right)/2 \tag{7}$$

The average local wall heat flux (q''_w) values was calculated by

$$q''_w = \left(q_{\max} + q_{\min}\right)/2 \tag{8}$$

The local Nusselt numbers (Nu_x) are then determined by

$$Nu_x = \left[q''_w / \left(T_w - T_b\right)\right] \times \left(D_h / k_f\right) \quad (9)$$

Constant wall temperature (T_w), fluid thermal conductivity (k_f) and hydraulic diameter (D_h) are assumed.

Once the Nusselt number of serpentine and straight path layouts are obtained, the enhancement factors can be determined from Equation (3). The pressure drop values are defined as thus:

$$e_f = \left(P_{o,m} - P_{i,m}\right)_{serpentine} / \left(P_{o,m} - P_{i,m}\right)_{straight} \quad (10)$$

Model Discretization

The ANSYS FLUENT solver utilised an element-based Finite Volume Method (FVM) that involves discretising the spatial domain with mesh, which serves to create finite volumes to conserve mass, momentum and energy. To improve the computational efficiency and accuracy, a swept hexahedral mesh was used for the discretising model. The mesh was extruded from the inlet along the axial path of the serpentine layout to produce the swept mesh, as shown in Figure 2. All the cells were set to quadrilateral shape. Edge division was used to specify the desired number of divisions within the edge.

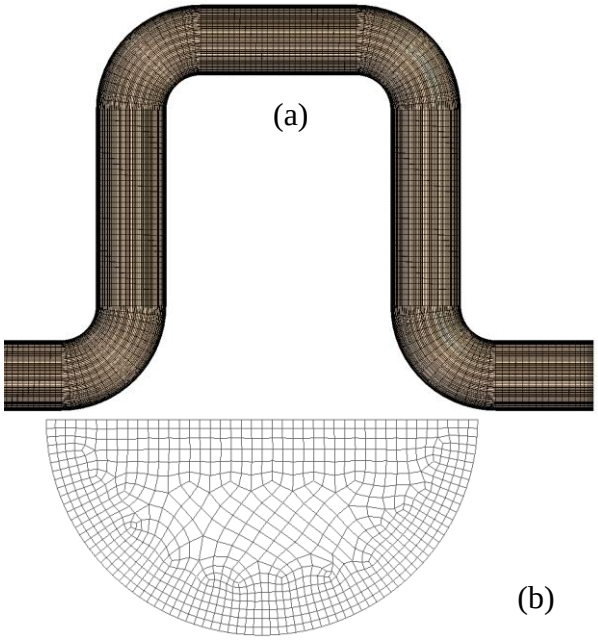

Figure 2. Mesh density (a) along axial direction and (b) on a cross-section.

RESULTS AND DISCUSSION

This section reports on the result for Nusselt number of straight transitional microchannel, enhancement factor of serpentine channel, and effect of Reynolds number in transitional serpentine microchannel.

Nusselt Number of Straight Transitional Microchannel

In this study, the obtained Nusselt number for a semi-circular cross-section straight transitional microchannel is about 3.567 under transitional flow. Compared to the value 3.323, there is an increase of 0.244 or 7.34% from the theoretical value [28]. Moreover, compared to the smallest value 3.221, there is a 10.74% increase [29]. One possible factor that attributes to these different values is the applied meshing approach. Rosaguti et al. utilised ICEM computational fluid dynamics to create a hexa-mesh or unstructured mesh, which is apparently different from the ANSYS Meshing approach in this study [28].

Figure 3 shows the Nusselt number at different locations along the channel. The Nusselt number is the highest at the inlet, then, it decreases gradually until the constant value. It reaches a constant value just before halfway of the 3 mm channel, which is approximately 0.6 mm from channel inlet.

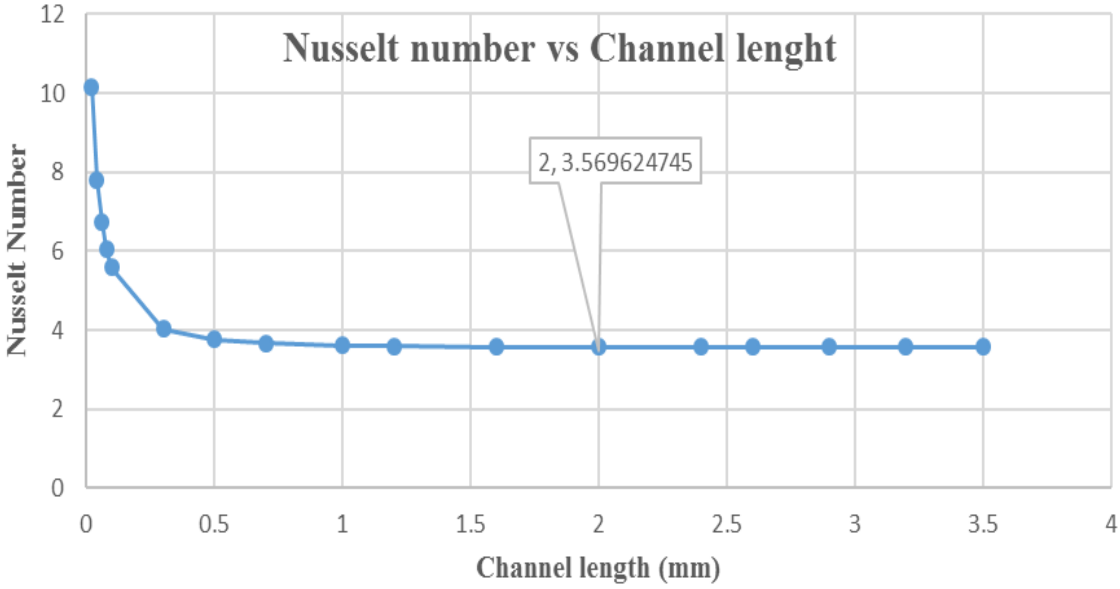

Figure 3. The obtained Nusselt number versus channel length.

In Figure 4(a), the temperature profile starts to develop from the channel entrance until it reaches the channel outlet. The change of temperature is obvious at the channel upstream, whereas, downstream shows almost a single concentration colour, which is the result of the bulk fluid temperature being close to the wall surface temperature. As heat transfer exists along the channel, the temperature profile keeps changing, even as the flow is fully developed.

Figure 5 shows that the velocity profile starts to form at the channel entrance. The velocity keeps growing towards the centre of channel until it is fully developed. Unlike the temperature profile that keeps increasing throughout the channel, there are no changes in the velocity profile when it is fully developed. The velocity magnitude for each layer remains constant until exiting the channel.

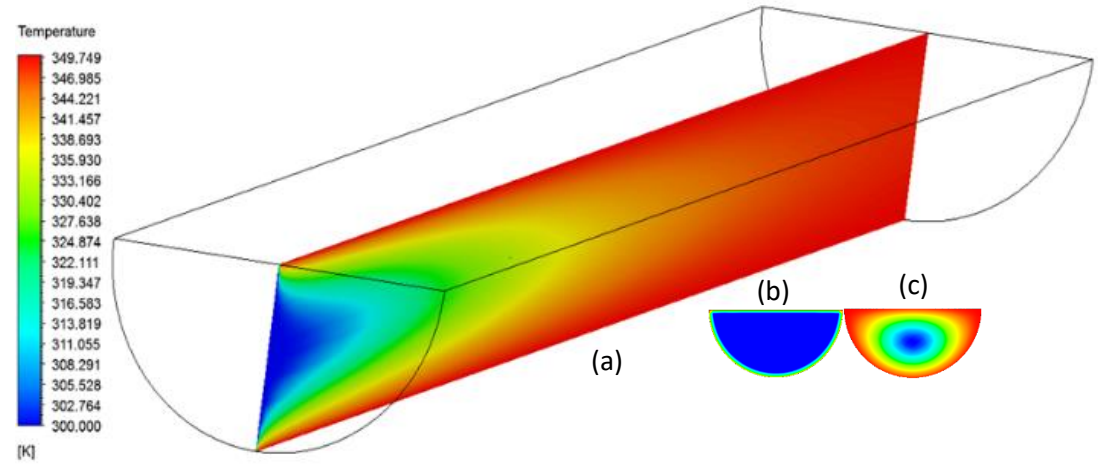

Figure 4. a) Sectional view of temperature boundary layer; b) Inlet channel temperature contour; c) Outlet channel temperature contour.

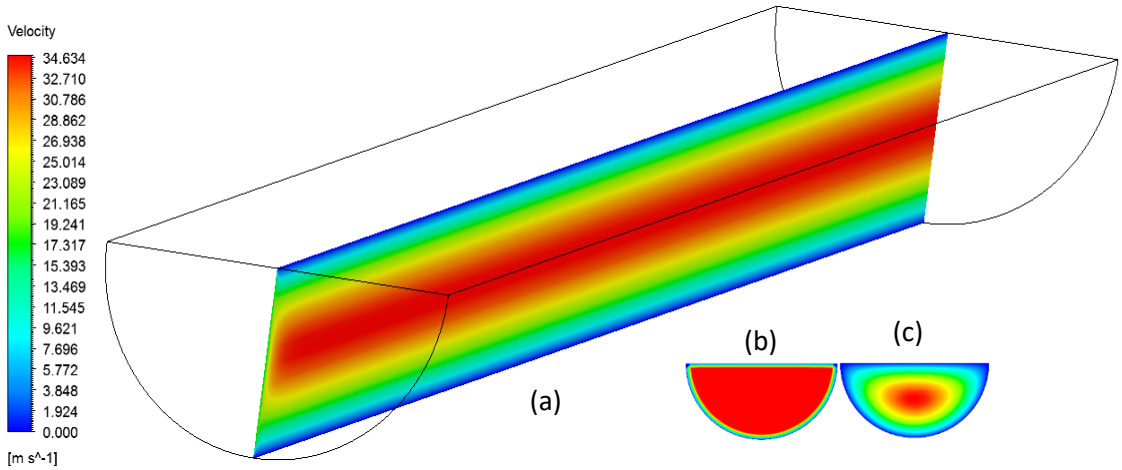

Figure 5. a) Sectional view of velocity boundary layer; b) Inlet channel velocity contour; c) Outlet channel velocity contour.

Enhancement factor of serpentine channel

Figure 6 shows that the effect of Reynolds number on fluid flow behaviour is very significant. At lower Reynolds numbers, the enhancement of heat transfer in the serpentine path, compared to straight path, are slightly increased with no apparent peak. The average enhancement factor with Reynolds number of 25 was found to be 0.99 because of the viscous forces being larger than the inertial forces.

For a Reynolds number of 100, planes 3, 9, 14 and 18 show the peak value of bend 1, 2, 3 and 4, respectively. By inspecting the curve, the enhancement factor decreases dramatically immediately after leaving the bends. This curve behaviour obeys the theoretical flow of fluid of serpentine channel as heat transfer decreases in the straight section.

As bend 1 and 3 are reinforcing bends, they show higher enhancement compared to bends 2 and 4. However, this condition is only applicable for Reynolds numbers up to 150 (Figure 6). Any further increase in Reynolds number causes the flow to become unsteady, in which case, bends 2 and 4 illustrate higher enhancement, compared to bends 1 and 3, which is theoretically not accurate.

Rosaguti et al. and Fourie reported that Reynolds numbers exceeding 450 tend to produce unsteady flow [28-29]. However, in this study, the flow becomes unsteady with Reynolds numbers greater than 150. Therefore, it shows that by decreasing the hydraulic diameter, the allowable Reynolds number of fluid steady flow is decreased.

The velocity contours shown in Figure 7 are in the fully developed section of the serpentine channel. It was observed that the rotational direction of Dean vortices alternates after every second bend, causing the bends to have different performance of heat transfer. After the fluid flows through bend 1, the vortices rotate in a reversed direction in the bend 2 vicinity, which causes weak heat transfer. Similarly, the reversal direction in bend 4 after bend 3 causes a reduction in heat transfer. As bends 2 and 3 have the same rotational direction, the strength of vortices is enhanced within the passage, causing bend 3 to have good heat transfer performance. Likewise, the rotational directions of bends 4 and 1 are in the same sense, which causes the heat transfer enhancement to be better in bend 1.

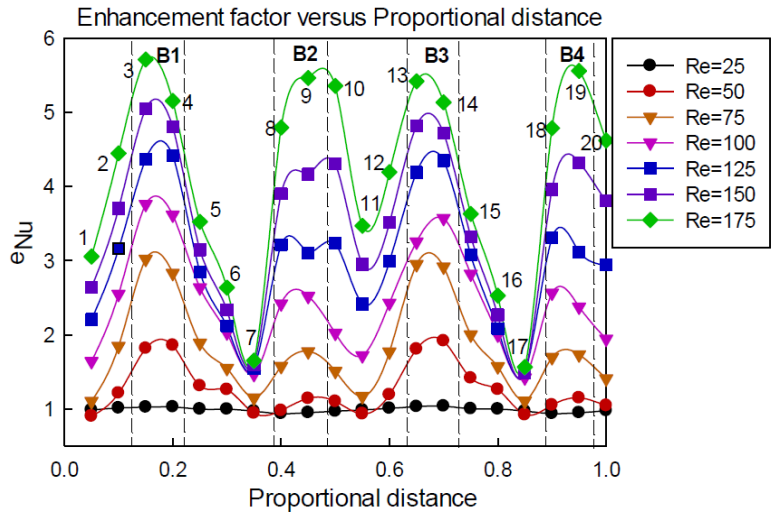

Figure 6. Heat transfer enhancement factor as a function of proportional distance within the transitional serpentine microchannel with $\mathbf{R_c/d}$ =1 and $\mathbf{L/d}$ =4.5 for *T* boundary condition. The dashed lines indicate the positions of each bend.

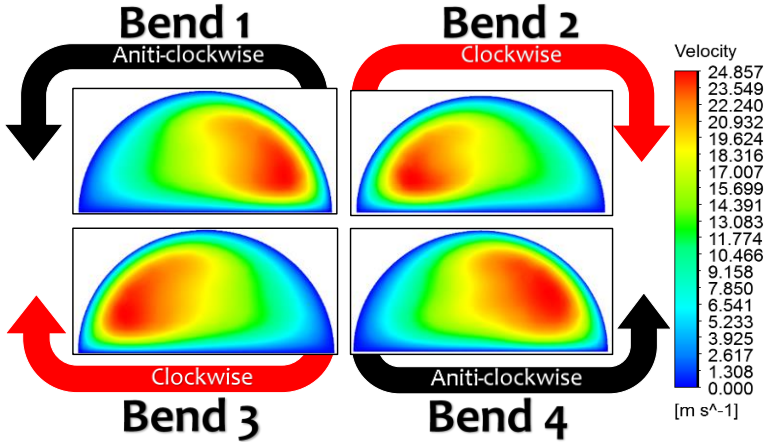

Figure 7. Velocity contour at the bends' downstream location for Reynolds number = 150.

In Figure 8, the velocity is found to be higher at bend 2 and bend 4. As these bends are cancelling bends, the rotational direction of the fluid that formed at the previous bend is disturbed, inducing the formation of vortices in the bends' vicinity. In Figure 8, the streamline suggests the vortices at cancelling bends are prominent over reinforcing bends; even with high vortices, bends 2 and 4 show lower heat transfer enhancement than bends 1 and 3. Therefore, the heat transfer enhancement is not dominated by the concentration of vortices; however, it is influenced by the mixing reaction at each bend, which infers that the vortices at the cancelling bends support mixing at the reinforcing bends, causing greater enhancement factors.

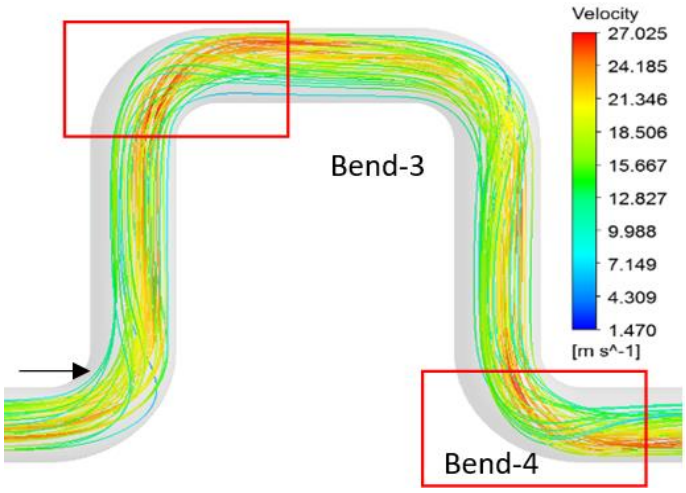

Figure 8. Fluid velocity streamlines in the studied channel.

Effect of Reynolds number

The effect of Reynolds number on average heat transfer enhancement is shown in Figure 9. When the value of Reynolds number increases, the heat transfer enhancement increases also. In addition, the effect of hydraulic diameter on heat transfer enhancement is displayed in Figure 9, showing that, with lower hydraulic diameter, the enhancement factor of the serpentine channel tends to increase higher than for larger hydraulic diameter. For instance, at the Reynolds number of 200, the simulation result is 75% larger than the value provided by Fourie [29]. Furthermore, the maximum Reynolds number for steady flow decreases with decreasing hydraulic diameter.

Convection heat transfer coefficient (h) was also determined using Equation (1). The results are as shown in Figure 10. At Reynolds number = 150, the calculated heat transfer coefficient is 768673.71 kJ/m^{2}K. However, the heat transfer coefficient as in Fourie's work with Reynolds number 400 is only 6731.45 kJ/m^{2}K [29], which indicates that the convective heat transfer in this study is better than that of the conventional microchannel.

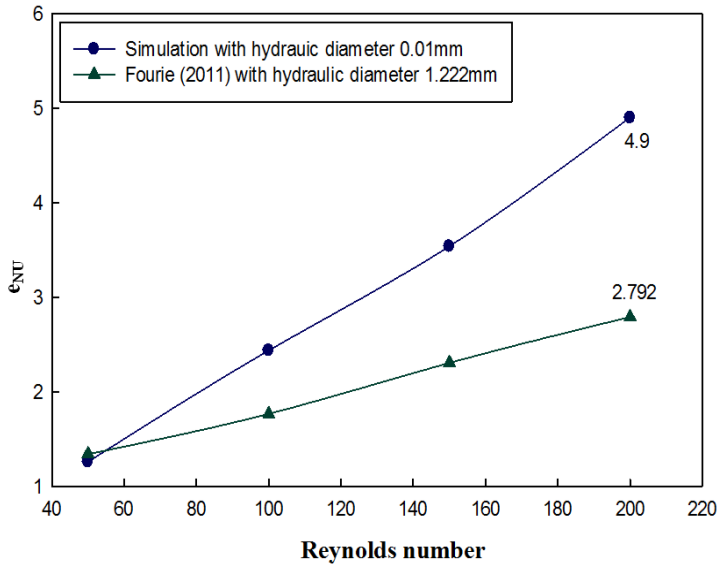

Figure 9. Comparison between simulation and theoretical results with different hydraulic diameters.

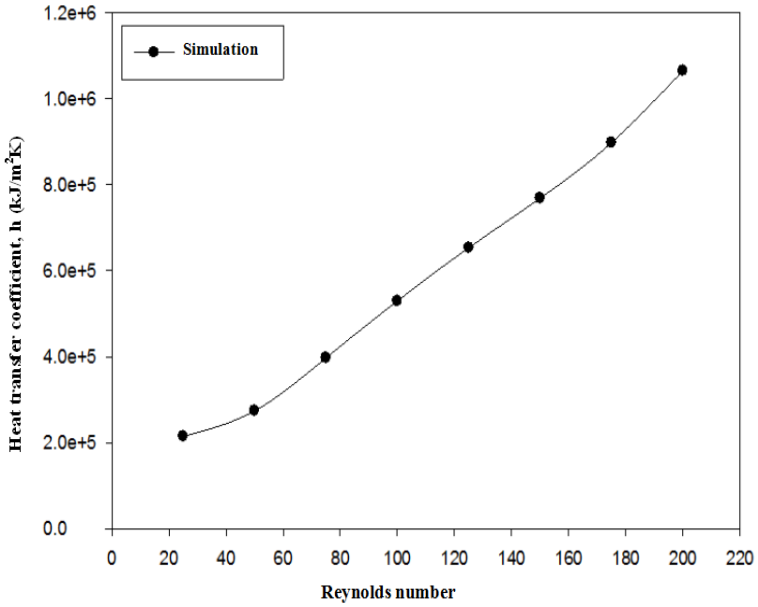

Figure. 10. Heat transfer coefficient for various Reynolds numbers.

In Figure 11, the pressure drop does not show any significant increase with increasing Reynolds number. At Reynolds number of 25, the pressure drop is about 0.8679, whereas, at Reynolds number of 175, the pressure drop is approximately 1.1134. Therefore, the pressure drop increases only by 0.2455. The pressure drop from the simulation has a lower value than that reported by Rosaguti et al. [28]. At lower Reynolds numbers (i.e. 25–100), the pressure drop of the straight channel is larger than for the serpentine path layout, which resulted in e_f <1. From Reynolds numbers of 125 onwards, the pressure drop of the serpentine layout is prominent over that of the straight channel (e_f >1). Therefore, the pressure drop is also dominated by the Reynolds number.

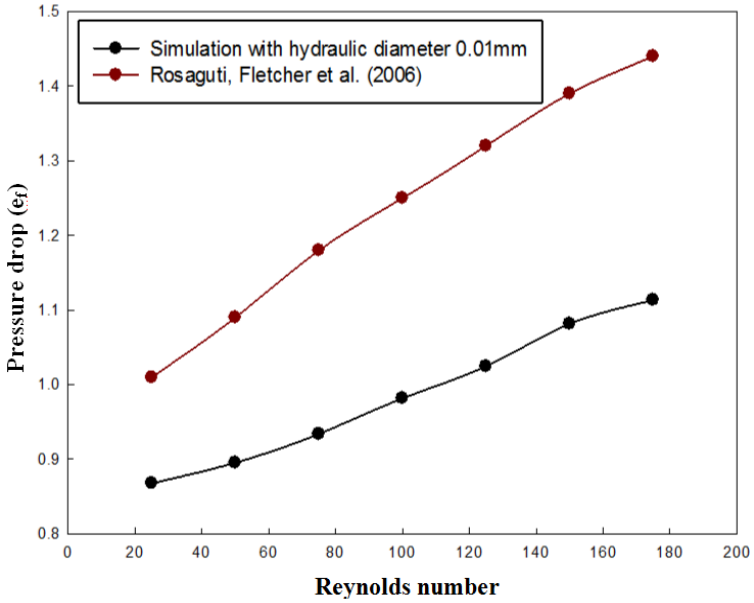

Figure 11. Effect of Reynolds number on pressure drop of serpentine channel.

CONCLUSION

A proposed methodology was used to investigate fully developed flow in both straight and serpentine channels of semi-circular cross-section with hydraulic diameter 10 µm. The effect of Reynolds number was more prominent on the heat transfer enhancement factor than on the pressure drop penalty. Increasing the Reynolds number led to a greater enhancement factor without incurring a large pressure drop penalty. For Reynolds number of 175, the obtained heat transfer coefficient in the study serpentine was greater than the theoretical value, which is 768673.71 kJ/m^{2}K, inferring that hydraulic diameter channel of 10 µm could improve greatly the heat transfer performance in microchannel heat exchanger application. However, physical experiment is needed to enhance the knowledge in this specific field.

ACKNOWLEDGEMENTS

The author would like to acknowledge the assistance and guidance provided by Swinburne University of Technology Sarawak.

REFERENCES

[1] Zhang P, Yao C, Ma H, Jin N, Zhang X, Lü H, Zhao Y. Dynamic changes in gas-liquid mass transfer during Taylor flow in long serpentine square microchannels. Chemical Engineering Science. 2018;182:17–27.

[2] Al-Neama AF, Khatir Z, Kapur N, Summers J, Thompson HM. An experimental and numerical investigation of chevron fin structures in serpentine minichannel heat sinks. International Journal of Heat and Mass Transfer. 2018;120:1213–1228.

[3] Al-Neama AF, Kapur N, Summers J, Thompson HM. An experimental and numerical investigation of the use of liquid flow in serpentine microchannels for microelectronics cooling. Applied Thermal Engineering. 2017;116:709–723.

[4] Filimonov R, Sorvari J. Numerical study on the effect of cross-section orientation on fluid flow and heat transfer in a periodic serpentine triangular microchannel. Applied Thermal Engineering. 2017;125:366–376.
[5] Imran AA, Mahmoud NS, Jaffal HM. Numerical and experimental investigation of heat transfer in liquid cooling serpentine mini-channel heat sink with different new configuration models. Thermal Science and Engineering Progress. 2018;6:128–139.
[6] Smakulski P, Pietrowicz S. A review of the capabilities of high heat flux removal by porous materials, microchannels and spray cooling techniques. Applied Thermal Engineering. 2016;104: 636–646.
[7] Tuckerman DB, Pease RFW. High-performance heat sinking for VLSI. IEEE Electron Device Letters. 1981;2:126–129.
[8] Missaggia L, Walpole JN, Liau ZL, Phillips RJ. Microchannel heat sinks for two-dimensional high-power-density diode laser arrays. IEEE Journal of Quantum Electron. 1989;25:1988–1992.
[9] Rahman MM, Gui F. Experimental measurements of fluid flow and heat transfer in microchannel cooling passage in a chip substract. Proceedings of the ASME International Electronics Packaging Conference. 1993;685–692.
[10] Wang BX, Peng XF. Experimental investigation on liquid forced convection heat transfer through microchannels. International Journal of Heat and Mass Transfer. 1994; 37:73–82.
[11] Peng XF, Peterson CP. Effect of thermofluid and geometrical parameters on convection of liquids through rectangular microchannels. International Journal of Heat and Mass Transfer. 1995;38:755–758.
[12] Peng XF, Peterson GP. Convective heat transfer and flow friction for water flow in microchannel structures. International Journal of Heat and Mass Transfer. 1996;39:2599–2608.
[13] Harms TM, Kazmierczak MJ, Gerner FM. Developing convective heat transfer in deep rectangular microchannels. International Journal of Heat and Fluid Flow. 1999;20:149–157.
[14] Mala CM, Li DQ. Flow characteristics of water in microtubes. International Journal of Heat and Fluid Flow. 1999;20:142–148.
[15] Lin QW, Gh MM, Li DQ. Pressure-driven water flow in trapezoidal silicon microchannels. International Journal of Heat and Mass Transfer. 2000;43:353–364.
[16] Ren L, Qu D, Li D. Interfacial electrokinetic effects on liquid flow in microchannels. International Journal of Heat and Mass Transfer. 2001;44:3125–3134.
[17] Celata GP, Cumo M, Gudlielmi M, Zummo G. Experimental investigation of hydraulic and single phase heat transfer in 0.130 mm capillary tube. Journal of Microsale Thermophysical Engineering. 2002;6:85–97.
[18] Wu HY, Cheng P. Experimental study of convective heat transfer in silicon microchannels with different surface conditions. International Journal of Heat and Mass Transfer. 2003;46:2547–2556.
[19] Baviere R, Ayela F, Person SL, Favre-Marinet M. An experimental study of water flow in smooth and rough rectangular micro-channels. ASME 2nd International Conference on Microchannels and Minichannels. 2004.
[20] Hao PF, He FH, Zhu KQ. Flow characteristics in a trapezoidal silicon microchannel. Journal of Micromechanics and Microengineering. 2005;15:1362–

1368.

[21] Shen S, Xu JL, Zhou JJ, Chen Y. Flow and heat transfer in microchannels with rough wall surface. Energy Conversion and Management. 2006;47:1311–1325.

[22] Jung JY, Kwak HY. Fluid flow and heat transfer in microchannels with rectangular cross section. International Journal of Heat and Mass Transfer. 2008;44:1041–1049.

[23] Wibel W, Ehrhard P. Experiments on the laminar/turbulent transition of liquid flows in rectangular microchannels. Journal of Heat Transfer Engineering. 2009;30:70–77.

[24] Mirmanto DBR, Kenning JS, Karayiannis TG. Pressure drop and heat transfer characteristics for single-phase developing flow of water in rectangular microchannels. Journal of Physics:Conference Series. 2012;395:1–14.

[25] Kottasamy A, Kadirgama K, Annamalai K, Mohanesan K, Ramasamy D, Noor MM. et al. Titanium oxide with nanocoolant for heat exchanger application. Journal of Mechanical Engineering and Sciences. 2017;11:2834–2844.

[26] Kandlikar SG, Grande WJ. Evolution of Microchannel Flow Passages-Thermohydraulic Performance and Fabrication Technology. Journal of Heat Transfer Engineering. 2003;24:3–17.

[27] Maina JN, West JB. Thin and strong! The bioengineering dilemma in the structural and functional design of the blood–gas barrier. Physiological Reviews. 2005;85;811–844.

[28] Rosaguti NR, Fletcher DF, Haynes BS. Laminar flow and heat transfer in a periodic serpentine channel with semi-circular cross-section. International Journal of Heat and Mass Transfer. 2006;47:2912–2923.

[29] Fourie JH. Thermal performance of periodic serpentine channels with semi-circular and triangular cross-sections. Potchesfstroom: North-West University; 2011.

[30] Venter J. The optimal hydraulic diameter of semicircular and triangular shaped channels for compact heat exchangers. Potchesfstroom: North-West University;2010.

[31] Rosaguti NR, Fletcher DF, Haynes BS. Low-Reynolds number heat transfer enhancement in sinusoidal channels. Chemical Engineering Science. 2007;62:694–702.

[32] Geyer PE, Fletcher DF, Haynes BS. Laminar flow and heat transfer in a periodic trapezoidal channel with semi-circular cross-section. International Journal of Heat and Mass Transfer. 2007;50:3471–3480.

[33] Liu JT, Peng XF, Yan WM. Numerical study of fluid flow and heat transfer in microchannel cooling passages. International Journal of Heat and Mass Transfer. 2007;50:1855–1864.